J. Fluid Mech. (1980), *vol.* 99, *part* 4, *pp.* 739–753
Printed in Great Britain

A strong interaction theory for the creeping motion of a sphere between plane parallel boundaries. Part 1. Perpendicular motion

By PETER GANATOS, SHELDON WEINBAUM AND ROBERT PFEFFER

The City College of The City University of New York, New York 10031

(Received 19 October 1979 and in revised form 15 February 1980)

This paper presents the first 'exact' solutions to the creeping-flow equations for the transverse motion of a sphere of arbitrary size and position between two plane parallel walls. Previous solutions to this classical Stokes flow problem (Ho & Leal 1974) were limited to a sphere whose diameter is small compared with the distance of the closest approach to either boundary. The accuracy and convergence of the present method of solution are tested by detailed comparison with the exact bipolar co-ordinate solutions of Brenner (1961) for the drag on a sphere translating perpendicular to a single plane wall. The converged series collocation solutions obtained in the presence of two walls show that for the best case where the sphere is equidistant from each boundary the drag on the sphere predicted by Ho & Leal (1974), using a first-order reflexion theory, is 40 per cent below the true value when the walls are spaced two sphere diameters apart and is one order-of-magnitude lower at a spacing of 1·1 diameters.

1. Introduction

The slow motion of a sphere in a viscous fluid between two plane parallel walls has important biological and engineering applications. The theory is needed to provide the hydrodynamic interaction parameter for modelling the diffusion of plasmalemma vesicles across endothelial cells lining the artery wall (Weinbaum & Caro 1976; Arminski, Weinbaum & Pfeffer 1980) and the diffusion of molecules across the intercellular space between adjacent cells. The more general theory, which includes the superposition of transverse and parallel motions, can be used to determine the motion of a particle passing through an electrostatic precipitator or the trajectory of a foreign particle in a lubricating bearing. Owing to the linearity of the governing differential equations and boundary conditions, the arbitrary planar motion of a sphere relative to two plane parallel walls can be separated into motions parallel and perpendicular to the confining boundaries. The solutions for the parallel motion are treated in part 2 (Ganatos, Pfeffer & Weinbaum 1980).

Despite its significance this classic low-Reynolds-number flow problem has eluded exact theoretical treatment for many years because of the lack of a natural co-ordinate system in which one could simultaneously satisfy the no-slip boundary conditions along the two walls and on the surface of the sphere. The existence of such a co-ordinate system made it possible for Brenner (1961) to obtain an exact series solution

0022-1120/80/4507-1710 $02.00

for the drag on a sphere translating perpendicular to a single plane wall. However the method used cannot be applied when two walls are present since the solution is based on the limiting case of a spherical bipolar series expansion in which the radius of one of the spheres is taken as infinitely large.

The only solutions currently available for the transverse motion of a sphere between two walls are the first-order method of reflexions results of Ho & Leal (1974) and the approximate analyses of Lorentz (1907) and Halow & Wills (1970) in which the contribution of each wall are simply added. The method of reflexions is an iterative series solution technique in which successive terms in the present application alternately satisfy boundary conditions on the sphere and on the confining walls. This series method gives accurate results using one or two reflexions only if both walls are far removed from the surface of the sphere. At close particle-to-wall spacings, the higher-order interaction effects become significant and the leading terms of the iterative series give a poor description of the particle–wall interactions. This behaviour causes the iterative series solution to converge very slowly. The study of Ho & Leal is part of a more general analysis in which these authors examine the effects of weak inertia on the lateral migration of a neutrally buoyant sphere in Couette or two-dimensional Poiseuille flow. The zeroth-order term of their perturbation series expansion in Reynolds number corresponds to the inertia-free Stokes flow problem considered in parts 1 and 2 of the present study.

The combined analytical–numerical solution procedure developed for the flow geometry treated in this study is a modification of the collocation series solution technique first developed by Gluckman, Pfeffer & Weinbaum (1971) for unbounded, axisymmetric multispherical Stokes flow and later extended to bounded flows by Leichtberg, Pfeffer & Weinbaum (1976) for co-axial chains of spheres in a tube. The present use of the technique is the first application of the general method to mixed spherical and planar co-ordinate geometries. This application requires that one first derive an expression for the disturbance produced by the perpendicular motion of an arbitrary spherical boundary along each of the confining walls and then be able to invert analytically the Fourier–Bessel transform of this disturbance so that the no-slip boundary conditions can be satisfied exactly along both confining walls simultaneously. In this manner, the original mixed co-ordinate, infinite domain boundary-value problem is reduced to a much simpler finite domain problem in which only the two infinite arrays of unknown coefficients describing the spherical disturbance need to be determined so as to satisfy the appropriate boundary conditions on the surface of the sphere. The latter problem is readily handled using the matrix-inversion boundary collocation technique described in Gluckman *et al.* (1971). As now demonstrated for axisymmetric and fully three-dimensional flows (Ganatos, Pfeffer & Weinbaum 1978) the boundary collocation procedure is a dramatic improvement over reflexion methods for strongly interacting Stokes flow since the disturbances from all boundaries are treated simultaneously rather than in an iterative fashion.

This paper is presented in four sections. Section 2 contains the formulation for the motion of a sphere perpendicular to two plane parallel walls. In § 3, the accuracy and convergence characteristics of the collocation series solution are examined by detailed comparison with the exact published results of Brenner (1961) for the motion of a sphere perpendicular to a single plane wall. Finally, in § 4 solutions are presented for the drag on a sphere of arbitrary size and position translating perpendicular to two

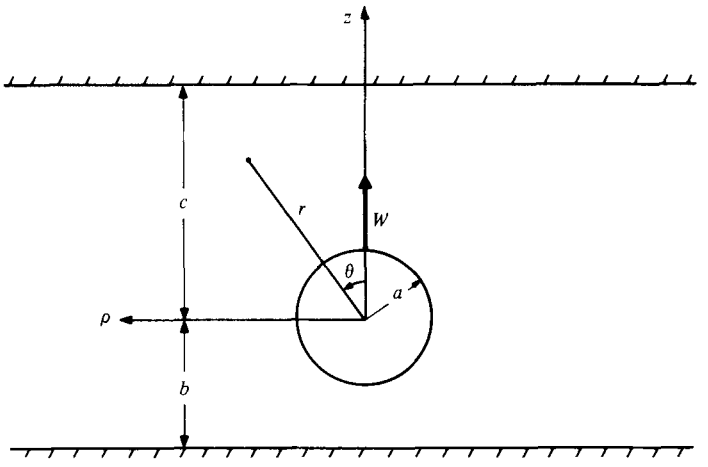

FIGURE 1. Geometry for the axisymmetric flow configuration.

plane parallel walls and the results compared, where available, with those obtained by the method of reflexions.

2. Mathematical formulation

We consider the creeping motion of a solid sphere of radius a moving with a constant velocity W in a viscous fluid perpendicular to two infinite plane parallel rigid boundaries whose distances from the centre of the sphere are b and c as shown in figure 1. The governing equations for the fluid motion are

$$\mu\nabla^2\mathbf{V} = \nabla p, \quad \nabla.\mathbf{V} = 0, \tag{2.1a, b}$$

where the symbols have their usual meaning. Owing to the axisymmetric nature of the flow, it is convenient to introduce the stream function ψ, satisfying (2.1b), which is given in cylindrical co-ordinates by

$$v_\rho = -\frac{1}{\rho}\frac{\partial\psi}{\partial z}, \quad v_z = \frac{1}{\rho}\frac{\partial\psi}{\partial\rho}. \tag{2.2a, b}$$

Here v_ρ and v_z are the radial and axial components of the fluid velocity respectively From (2.1a), the governing equation satisfied by the stream function is

$$D^2(D^2\psi) = 0, \tag{2.3}$$

where D^2 is the generalized axisymmetric Stokesian operator

$$D^2 = \frac{\partial^2}{\partial\rho^2} - \frac{1}{\rho}\frac{\partial}{\partial\rho} + \frac{\partial^2}{\partial z^2}. \tag{2.4}$$

For the geometry of the problem at hand, the stream function is linearly composed of two parts,

$$\psi = \psi_s + \psi_w. \tag{2.5}$$

The part ψ_s represents an infinite series containing all the simply separable solutions

of (2.3) in spherical co-ordinates which yield a vanishing fluid velocity as $r \to \infty$ and is given by Happel & Brenner (1973, p. 136) as

$$\psi_s = \sum_{n=2}^{\infty} [B_n r^{-n+1} + D_n r^{-n+3}] I_n(\xi). \tag{2.6}$$

Here $\xi = \cos\theta$ and $I_n(\xi)$ is the Gegenbauer function of the first kind of order n and degree $-\frac{1}{2}$; r and θ are spherical co-ordinates measured from the centre of the sphere (see figure 1); B_n and D_n are unknown constants which will be determined by satisfying the no-slip boundary conditions on the surface of the sphere in the presence of the confining walls.

The part ψ_w represents an integral of all the separable solutions of (2.3) in terms of cylindrical co-ordinates which produce finite velocities everywhere in the flow field and is given by the Fourier–Bessel integral

$$\psi_w = \int_0^{\infty} [A(\alpha)\, e^{\alpha z} + B(\alpha)\, e^{-\alpha z} + C(\alpha)\, \alpha z\, e^{\alpha z} + D(\alpha)\, \alpha z\, e^{-\alpha z}] \rho J_1(\alpha\rho)\, d\alpha. \tag{2.7}$$

Here $A(\alpha), \ldots, D(\alpha)$ are unknown functions of the separation variable α and J_1 is the Bessel function of the first kind of order unity. The integral rather than the infinite series form of the solution in cylindrical co-ordinates is required owing to the infinite non-periodic extent of the two planar boundaries. By proper choice of the unknown functions, the solution (2.7) is capable of exactly cancelling the disturbances produced by the sphere along the two confining walls.

Equation (2.5) is written in mixed co-ordinates; the cylindrical co-ordinate system (ρ, z) and spherical co-ordinate system (r, θ). In order to differentiate (2.6) and (2.7) and apply the no-slip boundary conditions along the two walls, it is necessary to relate the spherical co-ordinates to the cylindrical co-ordinate system. Using figure 1 the co-ordinate transformation is given by

$$r = (\rho^2 + z^2)^{\frac{1}{2}}, \quad \theta = \cos^{-1}\left(\frac{z}{[\rho^2 + z^2]^{\frac{1}{2}}}\right). \tag{2.8a, b}$$

Using (2.2), (2.5)–(2.8), the properties of Gegenbauer and Legendre functions and the chain rule, the radial and axial velocity components of the flow field are obtained:

$$v_\rho = -\frac{1}{\rho}\frac{\partial\psi}{\partial z} = \sum_{n=2}^{\infty} [B_n B_n'(\rho, z) + D_n D_n'(\rho, z)] + \int_0^{\infty} E(\alpha, z)\, \alpha J_1(\alpha\rho)\, d\alpha, \tag{2.9a}$$

$$v_z = \frac{1}{\rho}\frac{\partial\psi}{\partial\rho} = \sum_{n=2}^{\infty} [B_n B_n''(\rho, z) + D_n D_n''(\rho, z)] + \int_0^{\infty} F(\alpha, z)\, \alpha J_0(\alpha\rho)\, d\alpha, \tag{2.9b}$$

where

$$B_n'(\rho, z) = \frac{n+1}{(\rho^2 + z^2)^{\frac{1}{2}n}} \frac{1}{\rho} I_{n+1}\left(\frac{z}{[\rho^2 + z^2]^{\frac{1}{2}}}\right), \tag{2.10a}$$

$$D'_n(\rho,z) = \frac{n+1}{(\rho^2+z^2)^{\frac{1}{2}(n-2)}}\frac{1}{\rho}I_{n+1}\left(\frac{z}{[\rho^2+z^2]^{\frac{1}{2}}}\right) - \frac{2}{(\rho^2+z^2)^{\frac{1}{2}(n-1)}}\frac{z}{\rho}I_n\left(\frac{z}{[\rho^2+z^2]^{\frac{1}{2}}}\right), \quad (2.10b)$$

$$B''_n(\rho,z) = \frac{1}{(\rho^2+z^2)^{\frac{1}{2}(n+1)}}P_n\left(\frac{z}{[\rho^2+z^2]^{\frac{1}{2}}}\right), \quad (2.10c)$$

$$D''_n(\rho,z) = \frac{2}{(\rho^2+z^2)^{\frac{1}{2}(n-1)}}I_n\left(\frac{z}{[\rho^2+z^2]^{\frac{1}{2}}}\right) + \frac{1}{(\rho^2+z^2)^{\frac{1}{2}(n-1)}}P_n\left(\frac{z}{[\rho^2+z^2]^{\frac{1}{2}}}\right); \quad (2.10d)$$

$$E(\alpha,z) = -A(\alpha)\,e^{\alpha z} + B(\alpha)\,e^{-\alpha z} - C(\alpha)\,(1+\alpha z)\,e^{\alpha z} - D(\alpha)\,(1-\alpha z)\,e^{-\alpha z}, \quad (2.11a)$$

$$F(\alpha,z) = A(\alpha)\,e^{\alpha z} + B(\alpha)e^{-\alpha z} + C(\alpha)\,\alpha z\,e^{\alpha z} + D(\alpha)\,\alpha z\,e^{-\alpha z}; \quad (2.11b)$$

and P_n are Legendre functions of order n.

Application of the boundary conditions $v_\rho = v_z = 0$ along the two walls results in

$$\left.\begin{aligned}\int_0^\infty E(\alpha,z_i)\,\alpha J_1(\alpha\rho)\,d\alpha &= -\sum_{n=2}^{\infty}[B_n B'_n(\rho,z_i) + D_n D'_n(\rho,z_i)],\\ \int_0^\infty F(\alpha,z_i)\,\alpha J_0(\alpha\rho)\,d\alpha &= -\sum_{n=2}^{\infty}[B_n B''_n(\rho,z_i) + D_n D''_n(\rho,z_i)],\end{aligned}\right\} \quad i = 1,2, \quad (2.12)$$

where each of the above integral relations is applied at $z = z_i$ where z_i, $i = 1, 2$, has the values $-b$ and c respectively corresponding to each wall. The right-hand sides of (2.12) represent the disturbances produced by the sphere and felt on the two planar boundaries. These disturbances are functions only of the radial co-ordinate ρ. Inspection of (2.12) shows that the unknown functions E and F evaluated at the two walls are simply Hankel transforms of these disturbances. These equations may be inverted to give

$$\left.\begin{aligned}E(\alpha,z_i) &= -\int_0^\infty t\sum_{n=2}^{\infty}[B_n B'_n(t,z_i) + D_n D'_n(t,z_i)]\,J_1(\alpha t)\,dt,\\ F(\alpha,z_i) &= -\int_0^\infty t\sum_{n=2}^{\infty}[B_n B''_n(t,z_i) + D_n D''_n(t,z_i)]\,J_0(\alpha t)\,dt,\end{aligned}\right\} i = 1,2. \quad (2.13)$$

The integrals required in (2.13) are performed analytically as follows. Using the polynomial representations of the Gegenbauer and Legendre functions together with the result given by Erdelyi *et al.* (1954, vol. 2, p. 24)

$$\int_0^\infty \frac{x^{\nu+\frac{1}{2}}}{(x^2+a^2)^{\mu+1}}J_\nu(xy)\,(xy)^{\frac{1}{2}}\,dx = \frac{a^{\nu-\mu}y^{\mu+\frac{1}{2}}K_{\nu-\mu}(ay)}{2^\mu\Gamma(\mu+1)}, \quad (2.14)$$

$$\mathrm{Re}\,a > 0, \quad y > 0, \quad -1 < \mathrm{Re}\,\nu < 2\,\mathrm{Re}\,\mu + \tfrac{3}{2},$$

where K_ν is the modified Bessel function of the second kind, one can show by induction that

$$\int_0^\infty \frac{1}{(t^2+z_i^2)^{\frac{1}{2}n}}I_{n+1}\left(\frac{z_i}{[t^2+z_i^2]^{\frac{1}{2}}}\right)J_1(\alpha t)\,dt = \frac{1}{(n+1)!}\left(\frac{\alpha|z_i|}{z_i}\right)^{n-1}e^{-\alpha|z_i|}, \quad (2.15a)$$

$$\int_0^\infty \frac{1}{(t^2+z_i^2)^{\frac{1}{2}(n-2)}} I_{n+1}\left(\frac{z_i}{[t^2+z_i^2]^{\frac{1}{2}}}\right) J_1(\alpha t)\,dt$$
$$= \frac{1}{(n+1)!}\left(\frac{\alpha|z_i|}{z_i}\right)^{n-3}[(2n-1)\,\alpha|z_i| - n(n-2)]\,e^{-\alpha|z_i|}, \tag{2.15b}$$

$$\int_0^\infty \frac{t}{(t^2+z_i^2)^{\frac{1}{2}(n+1)}} P_n\left(\frac{z_i}{[t^2+z_i^2]^{\frac{1}{2}}}\right) J_0(\alpha t)\,dt = \frac{\alpha^{n-1}}{n!}\left(\frac{|z_i|}{z_i}\right)^n e^{-\alpha|z_i|}, \tag{2.15c}$$

$$\int_0^\infty \frac{t}{(t^2+z_i^2)^{\frac{1}{2}(n-1)}} P_n\left(\frac{z_i}{[t^2+z_i^2]^{\frac{1}{2}}}\right) J_0(\alpha t)\,dt$$
$$= \frac{\alpha^{n-3}}{n!}\left(\frac{|z_i|}{z_i}\right)^n [(2n-1)\,\alpha|z_i| - (n-1)^2]\,e^{-\alpha|z_i|}, \tag{2.15d}$$

$$\int_0^\infty \frac{t}{(t^2+z_i^2)^{\frac{1}{2}(n-1)}} I_n\left(\frac{z_i}{[t^2+z_i^2]^{\frac{1}{2}}}\right) J_0(\alpha t)\,dt = \frac{\alpha^{n-3}}{n!}\left(\frac{|z_i|}{z_i}\right)^n [(n-1) - \alpha|z_i|]\,e^{-\alpha|z_i|}. \tag{2.15e}$$

Direct application of these results to (2.13) gives

$$\left.\begin{aligned} E(\alpha, z_i) &= \sum_{n=2}^{\infty} [B_n \mathscr{B}_n^*(\alpha, z_i) + D_n \mathscr{D}_n^*(\alpha, z_i)], \\ F(\alpha, z_i) &= \sum_{n=2}^{\infty} [B_n \mathscr{B}_n^{**}(\alpha, z_i) + D_n \mathscr{D}_n^{**}(\alpha, z_i)], \end{aligned}\right\} \qquad i = 1, 2, \tag{2.16}$$

where

$$\mathscr{B}_n^*(\alpha, z_i) = -\int_0^\infty tB_n'(t, z_i)\,J_1(\alpha t)\,dt = -\frac{1}{n!}\left(\frac{\alpha|z_i|}{z_i}\right)^{n-1} e^{-\alpha|z_i|}, \tag{2.17a}$$

$$\mathscr{D}_n^*(\alpha, z_i) = -\int_0^\infty tD_n'(t, z_i)\,J_1(\alpha t)\,dt$$
$$= -\frac{1}{n!}\left(\frac{\alpha|z_i|}{z_i}\right)^{n-3}[(2n-3)\,\alpha|z_i| - n(n-2)]\,e^{-\alpha|z_i|}; \tag{2.17b}$$

$$\mathscr{B}_n^{**}(\alpha, z_i) = -\int_0^\infty tB_n''(t, z_i)\,J_0(\alpha t)\,dt$$
$$= -\frac{\alpha^{n-1}}{n!}\left(\frac{|z_i|}{z_i}\right)^n e^{-\alpha|z_i|}, \tag{2.17c}$$

$$\mathscr{D}_n^{**}(\alpha, z_i) = -\int_0^\infty {}''_n tD(t, z_i)\,J_0(\alpha t)\,dt$$
$$= -\frac{\alpha^{n-3}}{n!}\left(\frac{|z_i|}{z_i}\right)^n [(2n-3)\,\alpha|z_i| - (n-1)\,(n-3)]\,e^{-\alpha|z_i|}. \tag{2.17d}$$

Equations (2.16) and (2.17) give the E and F functions evaluated at the two walls in terms of the as yet unknown spherical coefficients B_n and D_n. To obtain the E and F functions at any value of z one must determine the unknown functions $A(\alpha), \ldots, D(\alpha)$ in (2.11a, b). The expressions for $E(\alpha, z_i)$ and $F(\alpha, z_i)$ obtained from (2.16) are substituted into (2.11), whose right-hand sides are evaluated at the two walls $z = -b, c$.

This gives rise to four linear algebraic equations which may be solved simultaneously to yield the unknown functions $A(\alpha), \ldots, D(\alpha)$. Once these functions are obtained, they are substituted back into (2.11a, b) to give the desired expressions for E and F. After a considerable amount of algebraic manipulation, one obtains

$$E(\alpha,z) = G_3(\sigma,\eta)\,E(\alpha,-b) - G_3(\eta,\sigma)\,E(\alpha,c) - G_1(\sigma,\eta)\,F(\alpha,-b) + G_1(\eta,\sigma)\,F(\alpha,c), \tag{2.18a}$$

$$F(\alpha,z) = -G_2(\sigma,\eta)\,E(\alpha,-b) + G_2(\eta,\sigma)\,E(\alpha,c) + G_4(\sigma,\eta)\,F(\alpha,-b) - G_4(\eta,\sigma)\,F(\alpha,c), \tag{2.18b}$$

where

$$G_{1,2}(\mu,\nu) = 4\tau\mu\nu\left[\frac{\sinh\mu}{\mu} \pm \frac{\sinh\tau}{\tau}\frac{\sinh\nu}{\nu}\right]\Big/\delta, \tag{2.19a}$$

$$G_{3,4}(\mu,\nu) = 4\tau\left\{\nu\left[\cosh\mu - \frac{\sinh\tau}{\tau}\frac{\sinh\nu}{\nu}\right] \pm \mu\left[\frac{\sinh\mu}{\mu} - \frac{\sinh\tau}{\tau}\cosh\nu\right]\right\}\Big/\delta. \tag{2.19b}$$

The subscripts 1, 3 and 2, 4 refer to the plus and minus sign in the right-hand sides of (2.19) respectively, μ and ν are dummy variables,

$$\delta = 4[\sinh^2\tau - \tau^2], \tag{2.20}$$

$$\sigma = \alpha(z+b), \quad \eta = \alpha(z-c) \tag{2.21a, b}$$

and

$$\tau = \alpha(b+c). \tag{2.21c}$$

The expressions for $E(\alpha,z)$ and $F(\alpha,z)$, still in terms of the unknown spherical coefficients B_n and D_n, are substituted into (2.9) to yield the local fluid velocity at any point in the flow. After some rearranging the result is

$$v_\rho = \sum_{n=2}^{\infty}\{B_n[B_n'(\rho,z) + \mathscr{B}_n'(\rho,z)] + D_n[D_n'(\rho,z) + \mathscr{D}_n'(\rho,z)]\}, \tag{2.22a}$$

$$v_z = \sum_{n=2}^{\infty}\{B_n[B_n''(\rho,z) + \mathscr{B}_n''(\rho,z)] + D_n[D_n''(\rho,z) + \mathscr{D}_n''(\rho,z)]\}, \tag{2.22b}$$

where

$$\begin{bmatrix}\mathscr{B}_n'(\rho,z)\\ \mathscr{D}_n'(\rho,z)\end{bmatrix} = \int_0^\infty \left\{G_3(\sigma,\eta)\begin{bmatrix}\mathscr{B}_n^*(\alpha,-b)\\ \mathscr{D}_n^*(\alpha,-b)\end{bmatrix} - G_3(\eta,\sigma)\begin{bmatrix}\mathscr{B}_n^*(\alpha,c)\\ \mathscr{D}_n^*(\alpha,c)\end{bmatrix}\right.$$
$$\left. - G_1(\sigma,\eta)\begin{bmatrix}\mathscr{B}_n^{**}(\alpha,-b)\\ \mathscr{D}_n^{**}(\alpha,-b)\end{bmatrix} + G_1(\eta,\sigma)\begin{bmatrix}\mathscr{B}_n^{**}(\alpha,c)\\ \mathscr{D}_n^{**}(\alpha,c)\end{bmatrix}\right\}\alpha J_1(\alpha\rho)\,d\alpha, \tag{2.23a}$$

$$\begin{bmatrix}\mathscr{B}_n''(\rho,z)\\ \mathscr{D}_n''(\rho,z)\end{bmatrix} = \int_0^\infty \left\{-G_2(\sigma,\eta)\begin{bmatrix}\mathscr{B}_n^*(\alpha,-b)\\ \mathscr{D}_n^*(\alpha,-b)\end{bmatrix} + G_2(\eta,\sigma)\begin{bmatrix}\mathscr{B}_n^*(\alpha,c)\\ \mathscr{D}_n^*(\alpha,c)\end{bmatrix}\right.$$
$$\left. + G_4(\sigma,\eta)\begin{bmatrix}\mathscr{B}_n^{**}(\alpha,-b)\\ \mathscr{D}_n^{**}(\alpha,-b)\end{bmatrix} - G_4(\eta,\sigma)\begin{bmatrix}\mathscr{B}_n^{**}(\alpha,c)\\ \mathscr{D}_n^{**}(\alpha,c)\end{bmatrix}\right\}\alpha J_0(\alpha\rho)\,d\alpha. \tag{2.23b}$$

The solution (2.22) satisfies the no-slip boundary conditions all along the two planar boundaries for each value of the index n and for any values of the coefficients B_n and D_n. The single integrals indicated by (2.23) must be performed numerically. In this regard, it should be noted that the expressions for the $G_1 - G_4$ functions given by

(2.19)–(2.21) are prone to large round-off errors as $\alpha \to 0$ and should be computed by their Taylor series for small values of α. Moreover, for large values of α, equations (2.19)–(2.21) produce machine overflows and their asymptotic formulas should be used.

The boundary conditions to be satisfied on the surface of the sphere, $r = a$, are

$$v_\rho = 0, \quad v_z = W, \tag{2.24a, b}$$

where W is the velocity with which the sphere is translating perpendicular to the walls. The boundary collocation technique developed by Gluckman *et al.* (1971) for applying boundary conditions on the sphere surface in axisymmetric flow is ideally suited for this purpose.

To satisfy the boundary conditions (2.24a, b) exactly on the surface would require the solution of the entire infinite array of unknown coefficients B_n and D_n. The collocation technique satisfies the boundary conditions at a finite number of discrete points† on the sphere's generating arc and truncates the infinite series into a finite one. The two unknown coefficients in each term in (2.22) permit one to satisfy the exact no-slip boundary at one discrete point on the sphere. If the no-slip boundary conditions are to be satisfied at M points on the generating arc of the sphere, the infinite series in (2.22) are truncated after the Mth term. This results in a set of $2M$ simultaneous linear algebraic equations for the $2M$ B_n and D_n unknown coefficients of the truncated solution which may be solved by any standard matrix reduction technique. Once these constants are determined, the solution for the stream function (2.5) and the velocity field (2.9) is completely known.

The force exerted by the fluid on the sphere is shown in Happel & Brenner (1973, p. 115) to be

$$F = \mu\pi \int_0^\pi r^3 \sin^3\theta \frac{\partial}{\partial r}\left[\frac{D^2\psi}{r^2\sin^2\theta}\right] r\, d\theta. \tag{2.25}$$

Performing the above integration, using (2.5)–(2.7) and the orthogonality properties of the Gegenbauer functions, one obtains the simple relation

$$F = 4\pi\mu D_2. \tag{2.26}$$

The drag force on the sphere translating perpendicular to the two confining walls can alternatively be expressed using the drag correction factor λ as

$$F = 6\pi\mu a W\lambda, \tag{2.27}$$

where λ represents the ratio of the force that the sphere experiences in the presence of the confining walls to the force it would experience moving with the same velocity through an unbounded quiescent fluid. Equating the two expressions for the drag force yields

$$\lambda = D_2/1{\cdot}5aW. \tag{2.28}$$

3. Solutions for the motion of a sphere perpendicular to a single plane wall

In this section, the accuracy and convergence characteristics of the collocation procedure applied to (2.22) will be determined by comparing solutions obtained using the present method with the exact solutions of Brenner (1961) for translation of a

† Each boundary point actually represents a ring on which the no-slip boundary conditions are satisfied owing to the axisymmetric nature of the problem.

sphere perpendicular to a single plane wall. In order to make this comparison, the influence of the second wall may be removed from the more general two-wall solution given in the previous section by taking the limit as $c \to \infty$ in (2.17) and (2.19). The functions required in the solution (2.23) reduce to

$$G_{1,2}(\sigma, \eta \to -\infty) = \mp \sigma e^{-\sigma}, \quad G_{1,2}(\eta \to -\infty, \sigma) = 0, \tag{3.1a, b}$$

$$G_{3,4}(\sigma, \eta \to -\infty) = (1 \mp \sigma) e^{-\sigma}, \quad G_{3,4}(\eta \to -\infty, \sigma) = 0; \tag{3.1c, d}$$

$$\mathscr{B}_n^*(\alpha, c \to \infty) = \mathscr{D}_n^*(\alpha, c \to \infty) = 0, \tag{3.2a, b}$$

$$\mathscr{B}_n^{**}(\alpha, c \to \infty) = \mathscr{D}_n^{**}(\alpha, c \to \infty) = 0. \tag{3.2c, d}$$

There are several schemes which may be used to select the boundary points on the sphere on which the no-slip boundary conditions are exactly satisfied. Two such schemes will now be examined in detail.

The most accurate lowest-order truncation solution for the viscous drag force is obtained by choosing the boundary point $\theta = \frac{1}{2}\pi$. This point is the most advantageous since it controls the projected area of the sphere normal to its direction of motion and also satisfies the no-slip boundary conditions on the largest ring (θ = constant) around the sphere. Unfortunately, an examination of the system of linear algebraic equations for the B_n and D_n coefficients shows that, when the $\theta = \frac{1}{2}\pi$ point is used, the coefficient matrix (2.22) becomes singular. To overcome this difficulty, the point $\theta = \frac{1}{2}\pi$ may be replaced by two closely adjacent points $\theta = \frac{1}{2}\pi \pm \epsilon$. The optimum value of ϵ is found by obtaining solutions for a single wall at various sphere-to-wall spacings with the boundary conditions being satisfied exactly at only the two points $\theta = \frac{1}{2}\pi \pm \epsilon$ ($M = 2$) for a sequence of diminishing values of ϵ. The largest value of ϵ for which convergence to a desired accuracy is obtained is then chosen. The results of these runs are presented in table 1. The bipolar co-ordinate parameter α in Brenner (1961) is related to the sphere–wall spacing via $\alpha = \cosh^{-1}(b/a)$. Examination of table 1 shows that the drag correction factor λ converges to five significant digits for all spacings considered in the table when $\epsilon \leqslant 0{\cdot}01°$. Consequently, ϵ was taken as $0{\cdot}01°$ in the computations which follow. Additional points were selected as mirror-image pairs about the plane $\theta = \frac{1}{2}\pi$ in order to preserve the geometric symmetry of the boundary about this plane.

One scheme for spacing these additional points is to divide the half-arc of the sphere into equal segments (e.g. for $M = 6$ use $\theta = 30°, 60°, 89{\cdot}99°, 90{\cdot}01°, 120°, 150°$). This scheme, which was used by Leichtberg, Pfeffer & Weinbaum (1976) for the problem of flow past a finite-length chain of spheres at the centre-line of a circular cylinder, favours the larger rings on which the no-slip boundary conditions are exactly satisfied by not specifying a boundary point at $\theta = 0$ or π. Using this collocation scheme, solutions for λ were obtained for various M and α and compared with the exact solutions of Brenner (1961). These results are presented in table 2. The table shows that the collocation solutions converge monotonically to the exact solution to five significant figures at all spacings tested. Convergence is very rapid at the larger spacings but becomes slow when the sphere is located immediately adjacent to the wall.

Another possible scheme for spacing the boundary points would be to include a boundary point at $\theta = 0$ (and π). The role of this point should be of increasing importance as the gap between the sphere and the wall is made very small. Leichtberg,

ϵ	$\alpha = 0{\cdot}5$ $b/a = 1{\cdot}13$	$\alpha = 1{\cdot}0$ $b/a = 1{\cdot}54$	$\alpha = 2{\cdot}0$ $b/a = 3{\cdot}76$	$\alpha = 3{\cdot}0$ $b/a = 10{\cdot}1$
10°	−3·5674	−2·5251	−1·4039	−1·1249
1°	−3·4885	−2·5000	−1·4030	−1·1249
0·1°	−3·4877	−2·4998	−1·4030	−1·1249
0·01°	−3·4877	−2·4997	−1·4030	−1·1249
0·001°	−3·4877	−2·4997	−1·4030	−1·1249

TABLE 1. Drag correction factor for a sphere translating perpendicular to a single plane wall, $M = 2$. Convergence tests for optimum ϵ.

M	$\alpha = 0{\cdot}5$ $b/a = 1{\cdot}13$	$\alpha = 1{\cdot}0$ $b/a = 1{\cdot}54$	$\alpha = 1{\cdot}5$ $b/a = 2{\cdot}35$	$\alpha = 2{\cdot}0$ $b/a = 3{\cdot}76$	$\alpha = 2{\cdot}5$ $b/a = 6{\cdot}13$	$\alpha = 3{\cdot}0$ $b/a = 10{\cdot}1$
2	−3·4877	−2·4997	−1·7728	−1·4030	−1·2202	−1·1249
4	−6·3569	−2·9842	−1·8359	−1·4128	−1·2220	−1·1252
6	−7·8347	−3·0309	−1·8374	−1·4129	−1·2220	−1·1252
8	−8·6423	−3·0356	−1·8375	−1·4129	—	—
10	−9·0189	−3·0360	−1·8375	—	—	—
12	−9·1693	−3·0361	—	—	—	—
14	−9·2237	−3·0361	—	—	—	—
16	−9·2424	—	—	—	—	—
18	−9·2486	—	—	—	—	—
20	−9·2507	—	—	—	—	—
22	−9·2514	—	—	—	—	—
24	−9·2516	—	—	—	—	—
26	−9·2517	—	—	—	—	—
28	−9·2518	—	—	—	—	—
30	−9·2518	—	—	—	—	—
Exact	−9·2518	−3·0361	−1·8375	−1·4129	−1·2220	−1·1252

TABLE 2. Convergence of λ for a sphere translating perpendicular to a single plane wall at various sphere-to-wall spacings.

Weinbaum, Pfeffer & Gluckman (1976) used this collocation scheme to obtain solutions in the near-collision limit for two adjacent spheres in a chain. Unfortunately, the coefficient matrix (2.22) again becomes singular if the points $\theta = 0$ or π are used. To overcome this problem a new set of trial runs was made with $\theta = \epsilon, \frac{1}{2}\pi \pm \epsilon, \pi - \epsilon$ ($M = 4$) for various values of ϵ. The results of these runs are shown in table 3. Again, it was found that λ converges to five significant digits for all spacings tested when $\epsilon \leqslant 0{\cdot}01°$. Additional boundary points were chosen in pairs as before (e.g. for $M = 6$ use $\theta = 0{\cdot}01°$, 45°, 89·99°, 90·01°, 135°, 179·99°). The results of this collocation scheme for various M are compared to the exact single-wall solutions at various spacings in table 4. Examination of table 4 reveals oscillatory convergence of λ to the exact solution to five significant digits for all spacings tested. Comparison between tables 2 and 4 shows that convergence of the latter collocation scheme is as rapid or more rapid than the previous one at all spacings. Even at $\alpha = 0{\cdot}5$ ($b/a = 1{\cdot}13$) only fourteen points are required to obtain the drag to an accuracy of 0·005 %. At larger spacings, convergence is even more rapid. Accuracy to four significant figures is achieved with only eight points at $\alpha = 1$ ($b/a = 1{\cdot}54$) and four points at $\alpha = 2$ ($b/a = 3{\cdot}76$).

In light of the above numerical tests, it appears that the second collocation scheme is the more efficient one and consequently will be used for the two-wall solutions to be presented in the next section.

ϵ	$\alpha = 0{\cdot}5$ $b/a = 1{\cdot}13$	$\alpha = 1{\cdot}0$ $b/a = 1{\cdot}54$	$\alpha = 2{\cdot}0$ $b/a = 3{\cdot}76$	$\alpha = 3{\cdot}0$ $b/a = 10{\cdot}1$
10°	−20·434	−3·1592	−1·4131	−1·1252
1°	−33·195	−3·1948	−1·4132	−1·1252
0·1°	−33·407	−3·1952	−1·4132	−1·1252
0·01°	−33·409	−3·1952	−1·4132	−1·1252
0·001°	−33·409	−3·1952	−1·4132	−1·1252

TABLE 3. Drag correction factor for a sphere translating perpendicular to a single plane wall, $M = 4$. Convergence tests for optimum ϵ.

M	$\alpha = 0{\cdot}5$ $b/a = 1{\cdot}13$	$\alpha = 1{\cdot}0$ $b/a = 1{\cdot}54$	$\alpha = 1{\cdot}5$ $b/a = 2{\cdot}35$	$\alpha = 2{\cdot}0$ $b/a = 3{\cdot}76$	$\alpha = 2{\cdot}5$ $b/a = 6{\cdot}13$	$\alpha = 3{\cdot}0$ $b/a = 10{\cdot}1$
4	−33·409	−3·1952	−1·8428	−1·4132	−1·2220	−1·1252
6	−14·902	−3·0399	−1·8374	−1·4129	−1·2220	−1·1252
8	−9·8323	−3·0360	−1·8375	−1·4129	—	—
10	−9·3260	−3·0361	−1·8375	—	—	—
12	−9·2603	−3·0361	—	—	—	—
14	−9·2513	—	—	—	—	—
16	−9·2511	—	—	—	—	—
18	−9·2515	—	—	—	—	—
20	−9·2517	—	—	—	—	—
22	−9·2517	—	—	—	—	—
24	−9·2518	—	—	—	—	—
26	−9·2518	—	—	—	—	—
Exact	−9·2518	−3·0361	−1·8375	−1·4129	−1·2220	−1·1252

TABLE 4. Convergence of λ for a sphere translating perpendicular to a single plane wall at various sphere-to-wall spacings with boundary points placed near $\theta = 0, \pi$.

4. Solutions for the motion of a sphere perpendicular to two plane parallel walls

In the previous section, solutions for the motion of a sphere perpendicular to a single plane wall were presented, tested for convergence and compared to exact published results. In this section, solutions will be presented for the motion of a sphere perpendicular to two plane parallel walls and compared with those obtained by the method of reflexions technique (Ho & Leal 1974).

Before presenting these results we shall first examine how the rate of convergence is affected by the introduction of the second planar boundary. The spherical solution (2.6) is now required to cancel the disturbances simultaneously produced by the presence of both walls on the surface of the sphere. It is therefore expected that more terms in the series (2.6) will be required to achieve convergence especially at close spacings where the disturbances are strongest. Table 5 shows the rate of convergence as a function of sphere-to-wall spacing b/a and sphere position $s = b/d$ where $d = b + c$. The column $s = 0$ corresponds to the single-wall solution while $s = 0{\cdot}5$ corresponds to the case where each wall is equidistant from the centre of the sphere. Each configuration is solved a number of times with increasing M until convergence is achieved to four significant figures. The starting value of M for a given case in table 5 is the

b/a	M	$s = 0{\cdot}1$	$s = 0{\cdot}2$	$s = 0{\cdot}25$	$s = 0{\cdot}3$	$s = 0{\cdot}4$	$s = 0{\cdot}5$
1·1	16	−11·46	−11·50	−11·56	−11·69	−12·48	−21·00
	18	−11·46	−11·50	−11·56	−11·69	−12·48	−21·02
	20	−11·46	−11·50	−11·56	−11·69	−12·48	−21·03
	22	−11·46	−11·50	−11·56	−11·69	−12·48	−21·03
1·5	8	−3·206	−3·223	−3·253	−3·313	−3·619	−4·779
	10	−3·206	−3·223	−3·253	−3·313	−3·619	−4·780
	12	−3·206	−3·223	−3·253	−3·313	−3·619	−4·780
2·0	6	−2·126	−2·135	−2·151	−2·182	−2·335	−2·789
	8	−2·126	−2·135	−2·151	−2·182	−2·335	−2·789
5·0	4	−1·285	−1·287	−1·290	−1·296	−1·325	−1·397
	6	−1·285	−1·287	−1·290	−1·296	−1·325	−1·397

TABLE 5. Convergence of two-wall solutions at various sphere positions s and sphere-to-wall spacings b/a.

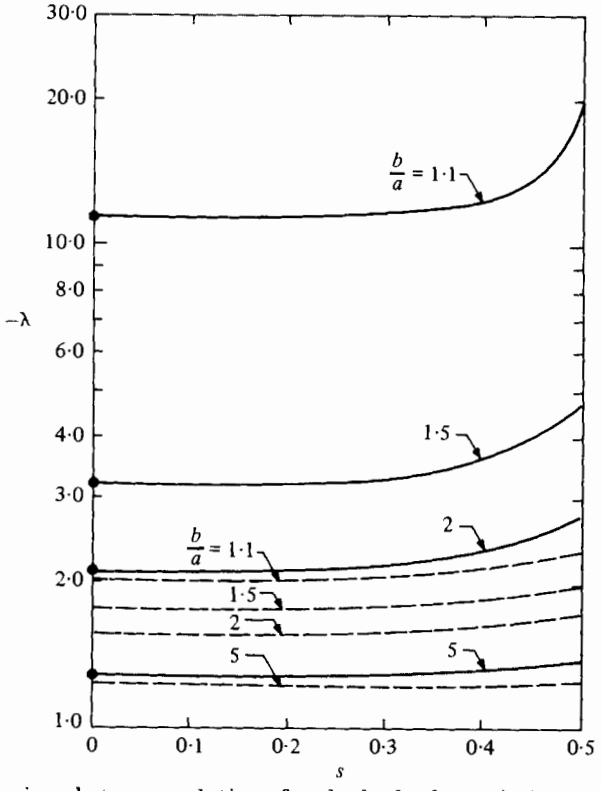

FIGURE 2. Comparison between solutions for the hydrodynamic interaction parameter λ for a sphere translating perpendicular to one or two plane parallel walls. ——, collocation (present study); — — —, Ho & Leal (1974), method of reflexions; ●, Brenner (1961) exact.

minimum value of M in table 4 which gives convergence to four significant figures. Examination of table 5 shows that introduction of the second wall has a surprisingly small adverse effect on the rate of convergence. The slowest rate of convergence is found at $s = 0{\cdot}5, b/a = 1{\cdot}1$, where the second wall is closest to the sphere and only four

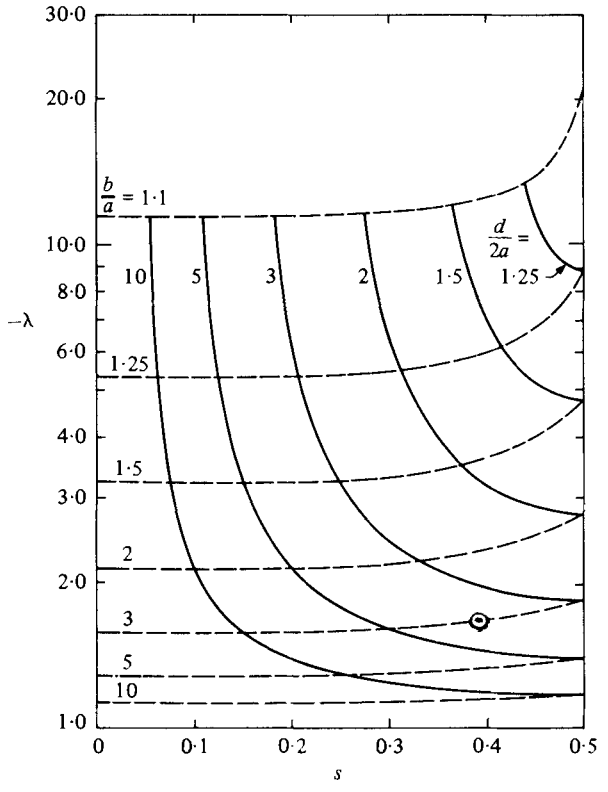

FIGURE 3. Drag on a sphere translating perpendicular to two plane parallel walls. ——, $d/2a$ = constant; — — —, b/a = constant.

additional points are required on the sphere to achieve four-digit accuracy for λ. For $b/a \geqslant 2$, no additional points are required.

Figure 2 shows a comparison of the 'exact' collocation solutions obtained in the present study with the first-order reflexion solutions obtained by Ho & Leal (1974) for the drag on a sphere translating perpendicular to two plane parallel walls. Also shown are the exact solutions obtained by Brenner (1961) for the motion of a sphere perpendicular to a single plane wall. The converged collocation solutions are in excellent agreement with the exact single-wall solutions of Brenner (1961) at all values of b/a. On the other hand, there is considerable error in the solutions obtained by the method of reflexions over the entire range of s. For example, at $s = 0{\cdot}5$ and $b/a = 1{\cdot}1$ the method of reflexions underestimates the drag on the sphere by a full order of magnitude. At $b/a = 2$ the error is as much as 40 per cent. It is only for spacings of $b/a = 5$ or greater that the method of reflexions begins to give meaningful results.

Figure 3 shows converged collocation solutions for the drag on a sphere translating perpendicular to two walls for several representative values of wall spacing to sphere diameter.† For a given wall-to-wall spacing, the sphere experiences minimum drag when it is located midway between the two walls and a drag that becomes infinite as the sphere approaches either of the boundaries. For $0 \leqslant s \leqslant 0{\cdot}25$ the presence of the

† Tables of numerical values of the drag force shown in figure 3 converged to four significant figures may be found in Ganatos (1979).

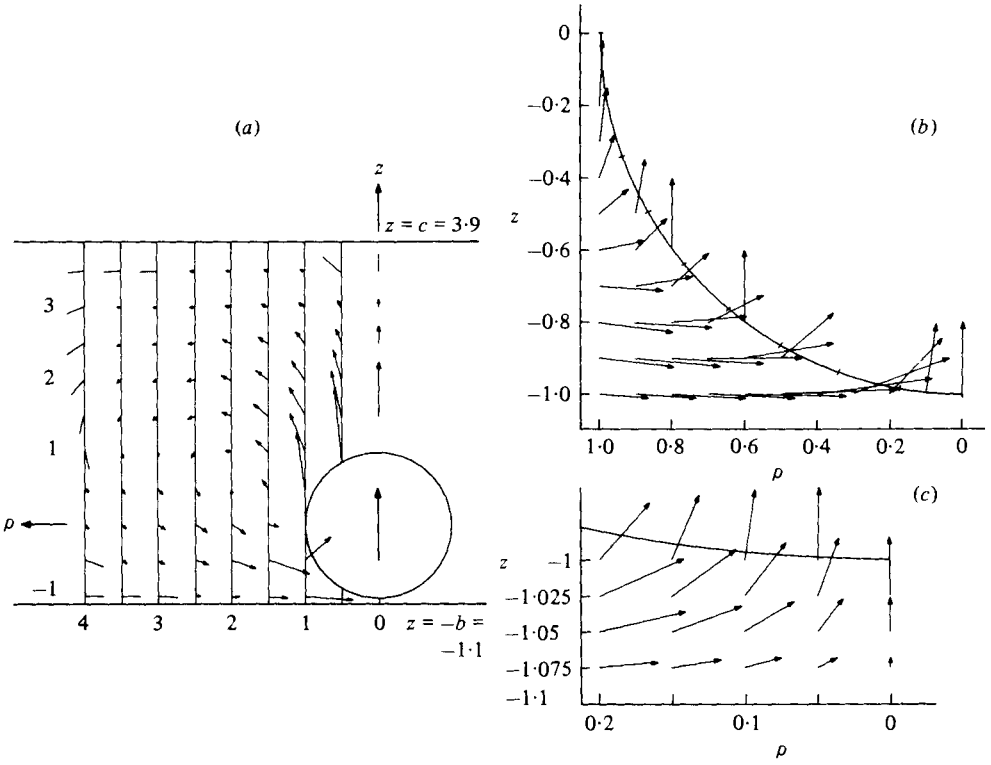

FIGURE 4. Velocity field induced by the translation of a sphere perpendicular to two plane walls; $d/2a = 2{\cdot}5$, $s = 0{\cdot}22$.

second wall has an insignificant effect on the drag of the sphere as demonstrated by the small slope of the curves b/a = constant (dashed lines).

Figure 4 shows a plot of the velocity field obtained using (2.22) for the case $d/2a = 2{\cdot}5$, $s = 0{\cdot}22$. The velocity vectors shown with arrowheads have been drawn to the same scale in all three views and show the magnitude and direction of the fluid motion. For cases where the magnitude of the velocity is too small to be visible on the scale shown, the direction of the fluid motion is shown by a straight line without an arrowhead at the indicated point. Figure 4*a* shows an overview of the flow field as the sphere is moving away from the nearer wall. The shape of the large eddy induced by the motion of the sphere is distorted by the presence of the confining walls. Figures 4(*b*, *c*) show a more detailed description of the flow field in the region $0 \leqslant \rho \leqslant 1$, $-1 \leqslant z \leqslant 0$ and $0 \leqslant \rho \leqslant 0{\cdot}2$, $-1{\cdot}1 \leqslant z \leqslant -1$ respectively. In this region the flow is required to make a 90° bend and the magnitude of the fluid velocity may even exceed the sphere velocity. Also shown in figure 4(*b*) is the location of the boundary points used on the surface of the sphere for this particular run ($M = 20$). The no-slip boundary conditions are satisfied exceedingly well along the entire surface of the sphere.

The calculations for the results presented in this paper were performed on an AMDAHL 470/V6 computer. The bulk of the computation time was used in the numerical evaluation of the integrals (2.23). Actual running times to determine the drag and the B_n and D_n velocity coefficients in (2.22) for one configuration were found to be $\frac{1}{2}M^2$ s at most spacings. At the largest sphere-to-wall spacings, computation times increased by about a factor of three due to the slower convergence of the integrals.

The authors wish to thank the National Science Foundation for supporting this research under grant ENG 75-19243 and The City University of New York Computer Center for the use of their facilities. The above work has been performed in partial fulfilment of the requirements for the Ph.D. degree of P. Ganatos from The School of Engineering of The City College of The City University of New York.

REFERENCES

ARMINSKI, L., WEINBAUM, S. & PFEFFER, R. 1980 *J. Theor. Biol.* (in press).

BRENNER, H. 1961 *Chem. Engng Sci.* **16**, 242.

ERDELYI, A., MAGNUS, W., OBERHETTINGER, F. & TRICOMI, F. G. 1954 *Tables of Integral Transforms*, vol. 2. McGraw-Hill.

GANATOS, P. 1979 Ph.D. dissertation, City University of New York.

GANATOS, P., PFEFFER, R. & WEINBAUM, S. 1978 *J. Fluid Mech.* **84**, 79.

GANATOS, P., PFEFFER, R. & WEINBAUM, S. 1980 *J. Fluid Mech.* **99**, 755–783.

GLUCKMAN, M. J., PFEFFER, R. & WEINBAUM, S. 1971 *J. Fluid Mech.* **50**, 705.

HALOW, J. S. & WILLS, G. B. 1970 *A.I.Ch.E. J.* **16**, 281.

HAPPEL, J. & BRENNER, H. 1973 *Low Reynolds Number Hydrodynamics*, 2nd edn. Noordhoff.

HO, B. P. & LEAL, L. G. 1974 *J. Fluid Mech.* **65**, 365.

LEICHTBERG, S., PFEFFER, R. & WEINBAUM, S. 1976 *Int. J. Multiphase Flow* **3**, 147.

LEICHTBERG, S., WEINBAUM, S., PFEFFER, R. & GLUCKMAN, M. J. 1976 *Phil. Trans. Roy. Soc.* A **282**, 585.

LORENTZ, H. A. 1907 *Abhand. Theor. Phys.* **1**, 23.

WEINBAUM, S. & CARO, C. G. 1976 *J. Fluid Mech.* **74**, 611.